Theoretical investigation of vibrational and isotopic properties of iron (oxyhydr)oxides
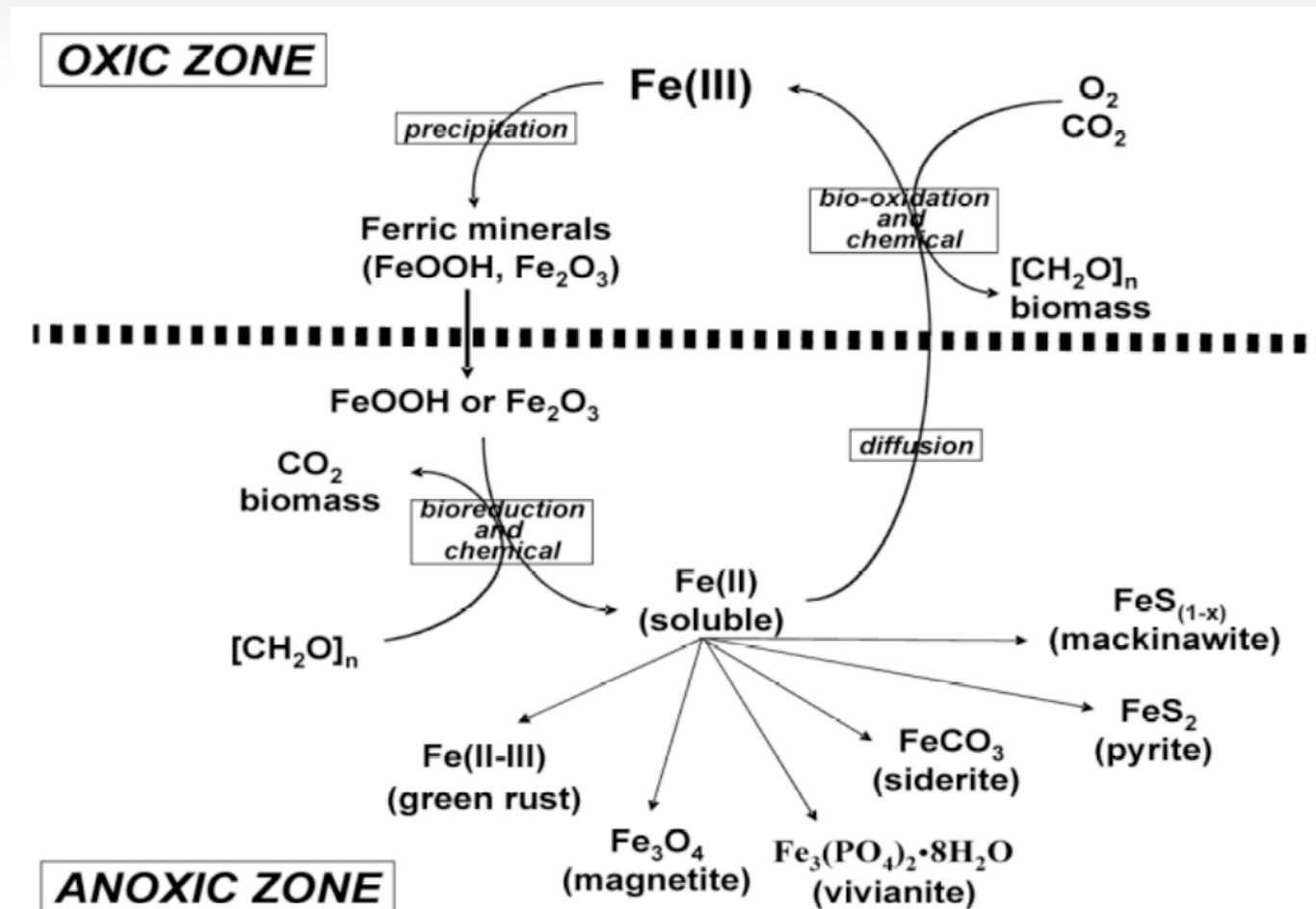
Marc Blanchard & Etienne Balan
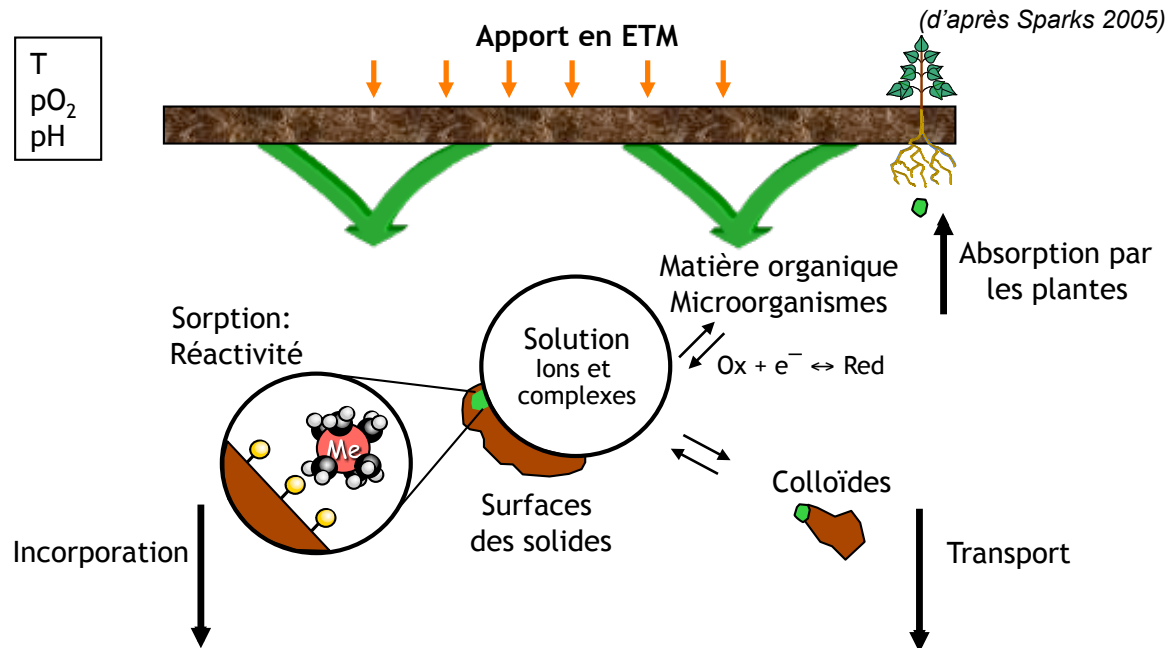
- Iron is the 4th most abundant element in the continental crust (5.1 wt%)

- 2 oxidation states (II, III)

Cornell RM, Schwertman U (2003) The iron oxides. Wiley-VCH, pp. 664

Chemical reactions at the interfaces between iron (oxyhydr)oxides and water play an important role in numerous natural processes:

• Biological availability (essential nutriment)
• Redox processes (weathering, soil formation, BIF)
• Fate and transport of environmental contaminants


Laterite, Brazil (IMPMC)

Apport en ETM

(d'après Sparks 2005)

T
pO$_2$
pH

Sorption:
Réactivité

Me

Incorporation

Solution
Ions et
complexes

Surfaces
des solides

Matière organique
Microorganismes

Ox + e$^-$ ↔ Red

Colloïdes

Absorption par
les plantes

Transport

Acid mine drainage, Ohio
(Cornell and Schwertmann 2003)

Iron isotope geochemistry

MC-ICP-MS (labo GET)

^{54}Fe (5.84 %), ^{56}Fe (91.76 %),
^{57}Fe (2.12 %), ^{58}Fe (0.28 %)

$\Rightarrow$ **Proxy complementary to traditional stable isotopes**

The most important Fe isotope fractionations occur in low-T environments and with redox gradients.
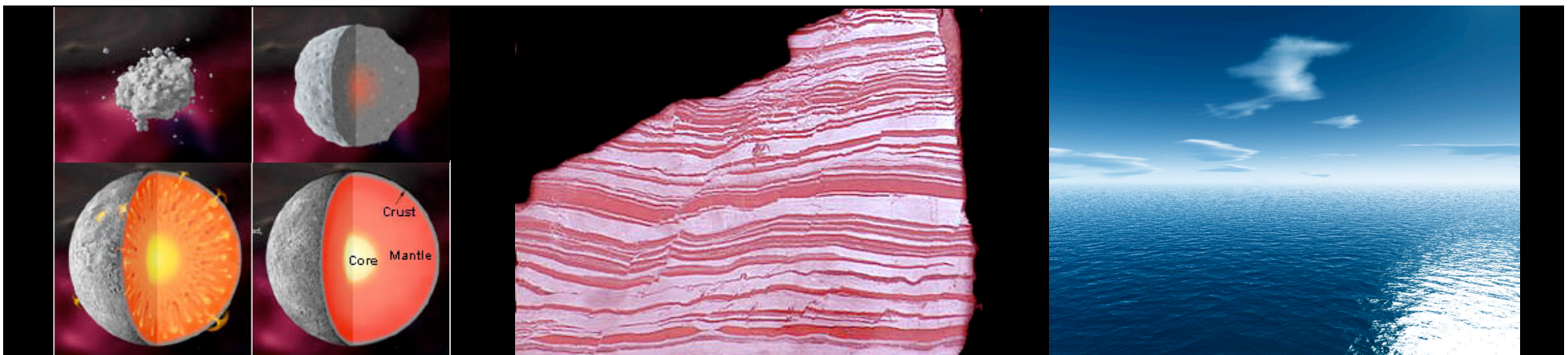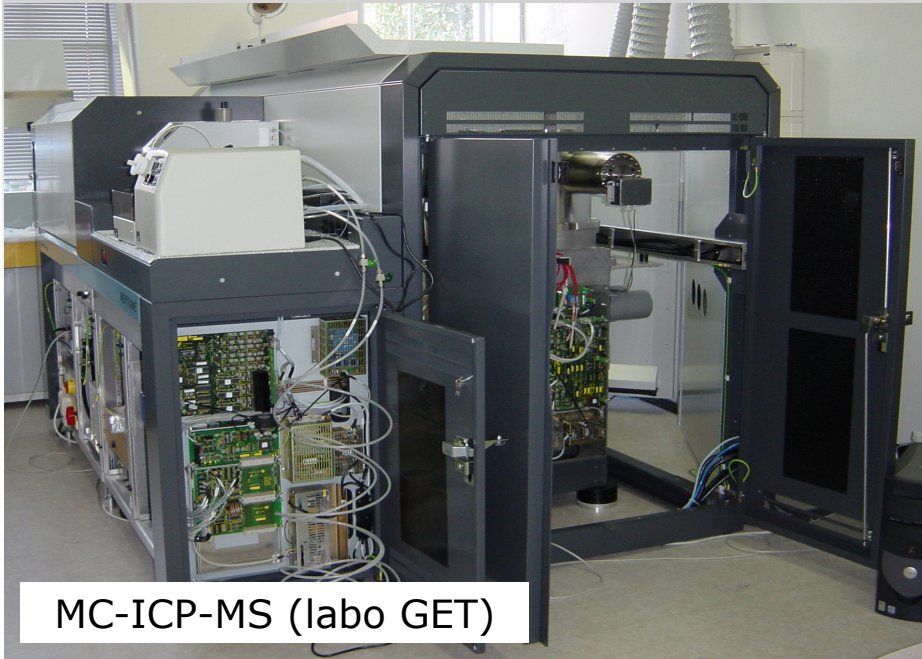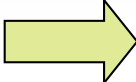

Planetary formation

Banded Iron Formation

Redox evolution of the ocean

An essential basis for interpreting isotopic compositions in natural samples
is to know the equilibrium isotopic fractionation factors
Mass-dependent equilibrium isotopic fractionation is controlled by
vibrational properties

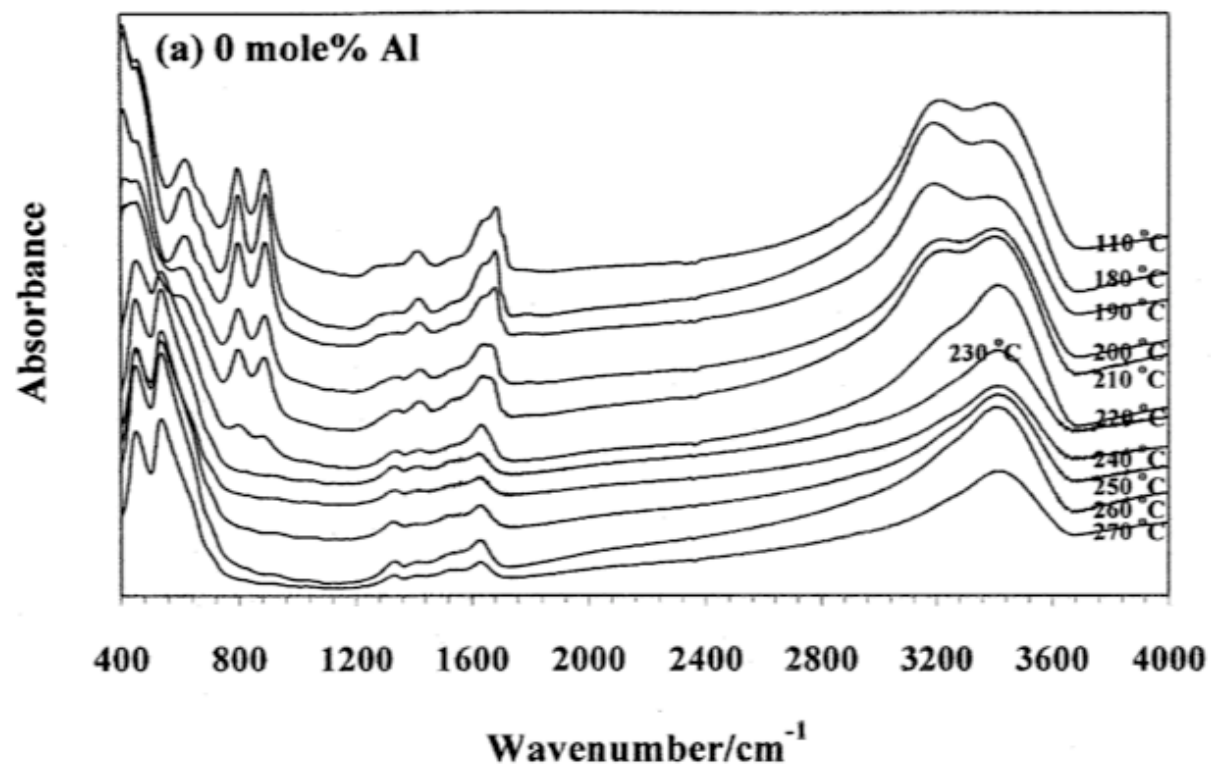⟹ Need a good description of the vibrational properties (IR, Raman)

For iron (oxyhydr)oxide, occurring most of the time as finely divided minerals,
IR spectroscopy is a technique of choice for the identification, for tracking
mineral transformations, but also for providing information about the
composition, the structural defects, the particle shape...

⟹ Theoretical modeling of IR spectra is useful

Transformation of goethite to hematite

(a) 0 mole% Al

110 °C
180 °C
190 °C
200 °C
210 °C
220 °C
230 °C
240 °C
250 °C
260 °C
270 °C

Absorbance

Wavenumber/cm^{-1}

400 800 1200 1600 2000 2400 2800 3200 3600 4000

(Ruan et al. 2002, *Spectrochim Acta*)

Goethite-Hematite, Lubéron
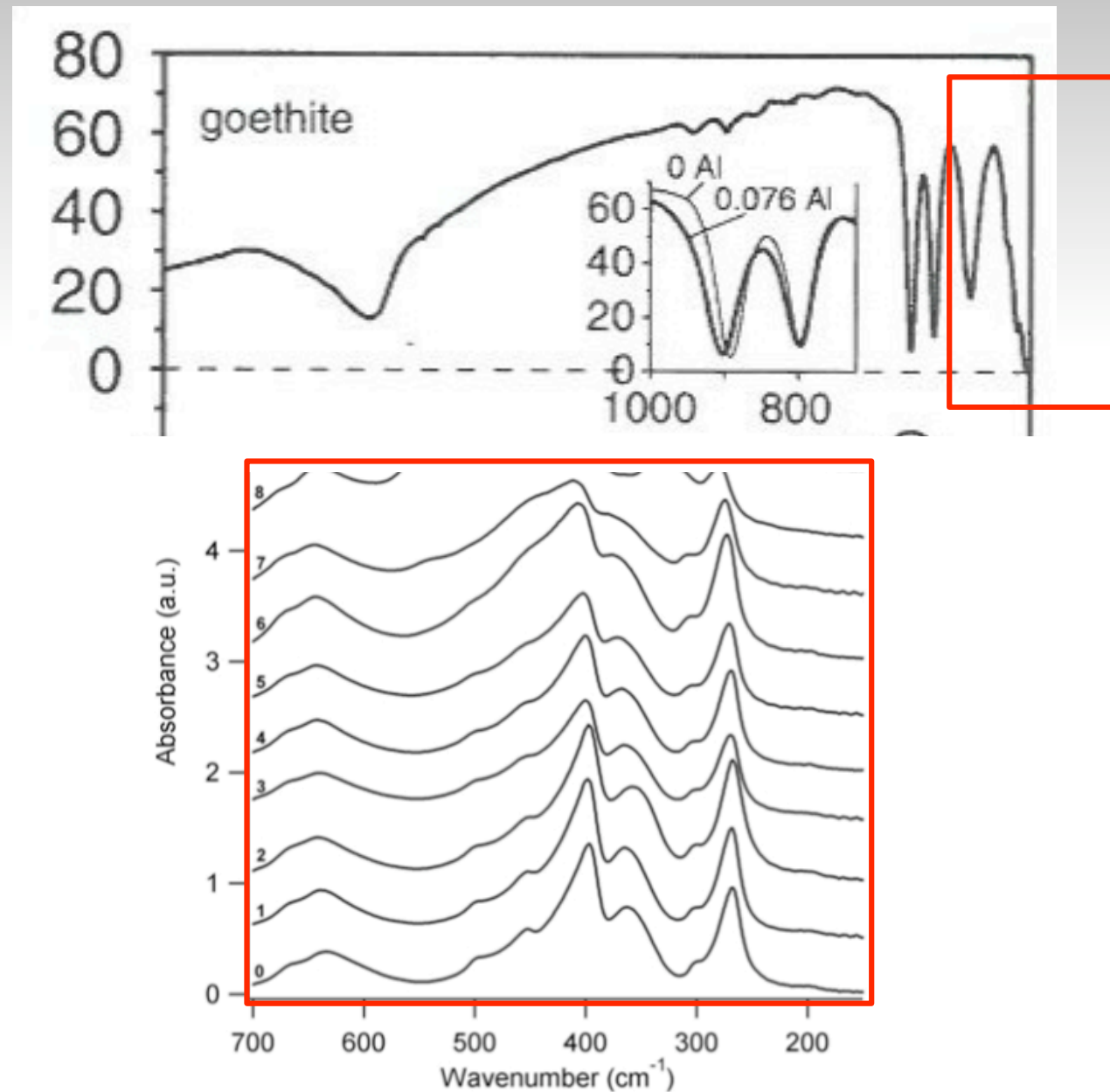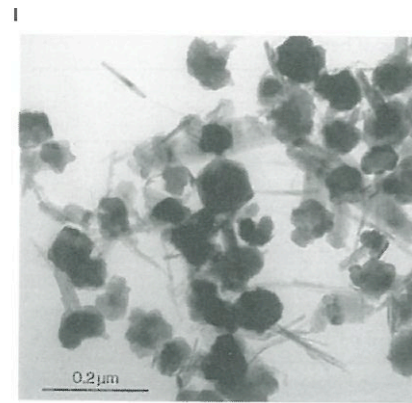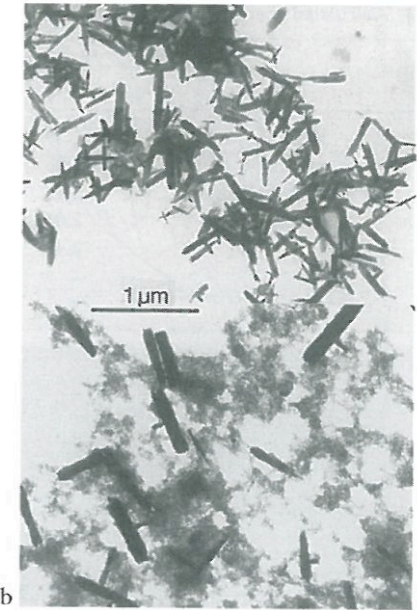(Cornell and Schwertmann 2003)

Al-bearing goethites

FIG. 4. IR spectra of Al-bearing goethites (see Table 2 for compositions of samples).
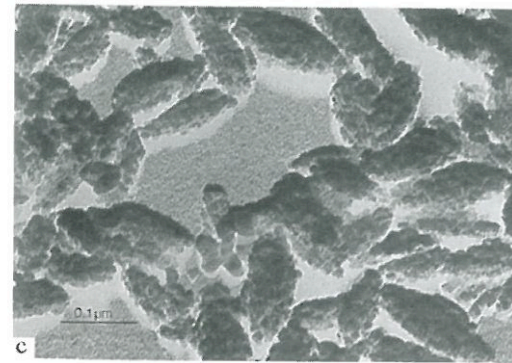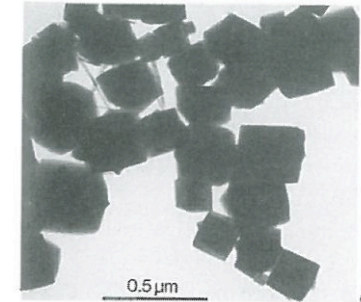
(Blanch et al. 2008, *Miner Mag*)

Hematite morphologies
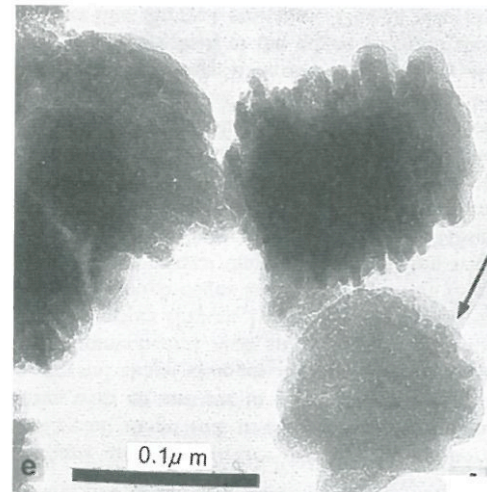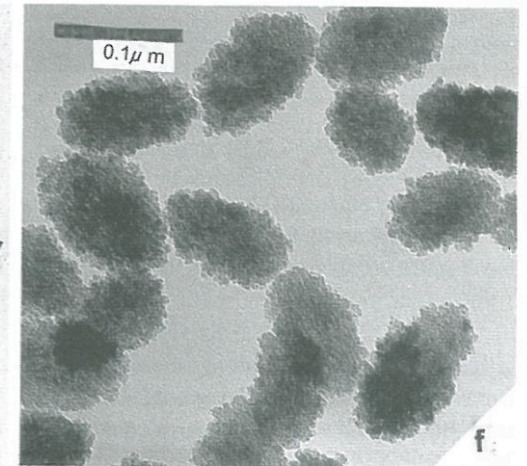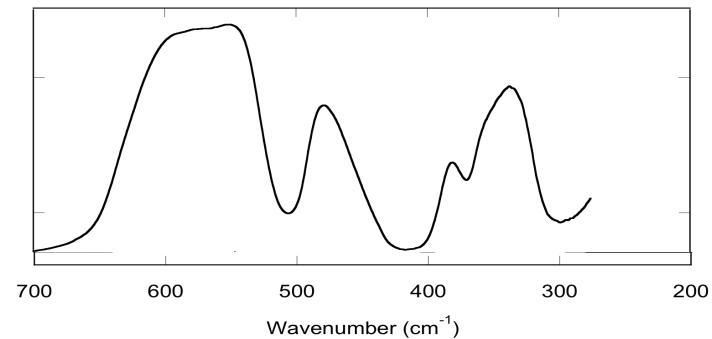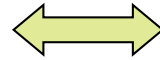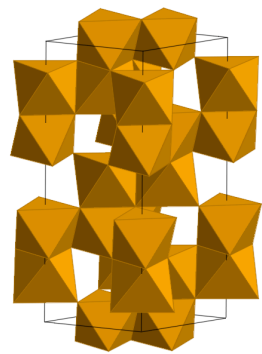

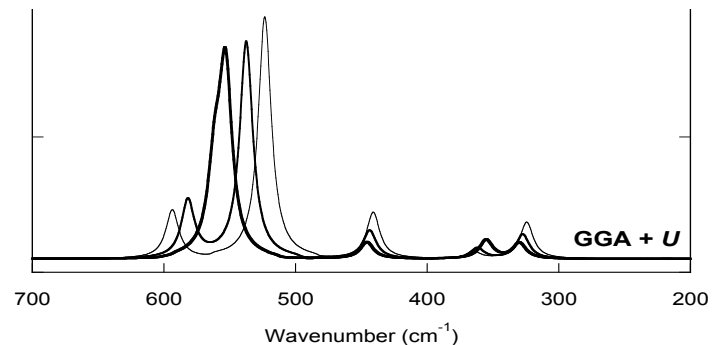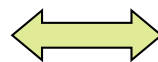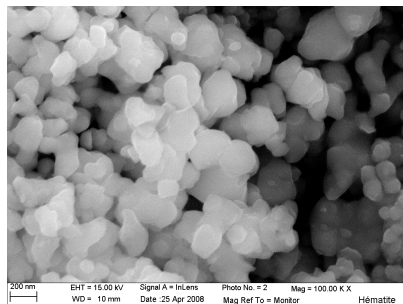(Cornell and Schwertmann 2003)

Theoretical modeling of IR spectra

In the interpretation of IR spectra, first-principles calculations are useful for:

- finding unambiguous relations beween IR spectrum, vibrational modes
and crystal structure

-determining the contribution of actual features of mineral samples
(e.g. particle shape, defects) to their IR spectrum

For a solid...
The induced polarisation is proportional to the macroscopic electric field existing in the material:

$$4\pi\, \boldsymbol{P}(\omega) = (\varepsilon(\omega) - 1)\, \boldsymbol{E}(\omega)$$

where $\varepsilon(\omega)$ is the dielectric tensor

An approach in two steps :

First-principles calculation
DFT

Classical electromagnetic model

CRYSTAL → dielectric tensor $\varepsilon(\omega)$ → IR SPECTRUM
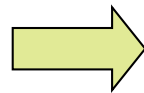
- GGA (PBE)
- planewaves, pseudo-potentials
- PWscf, CASTEP

- experimental geometry
- sample micro-structure
- ...

Calculation of the low-frequency dielectric tensor $\varepsilon(\omega)$

$$\varepsilon_{ij}(\omega) = \varepsilon_{ij}(\infty) + \frac{4\pi}{\Omega_0}\sum_m \frac{S_{m,ij}}{\omega_m^2-(\omega+i\Gamma)^2}$$

$\uparrow$ electronic $\qquad\qquad\qquad \uparrow$ ionic

$$S_{m,ij} = \left(\sum_{\tau,i'} Z^*_{ii',\tau}\, U_m(\tau,i')\right)\left(\sum_{\tau',j'} Z^*_{jj',\tau'}\, U_m(\tau',j')\right)$$

Γ damping coefficient

$\varepsilon(\infty)$ electronic dielectric tensor
Z^* Born effective charge tensors
U_m transverse normal modes
ω_m transverse vibrational frequencies

calculated using DFPT: second derivatives of total energy w.r.t. atomic displacements and/or macroscopic electric field

- harmonic approximation, athermal limit
- vibrational modes at the center of Brillouin zone
- accuracy: effective charges ~10 %; frequencies ~ 3 %;
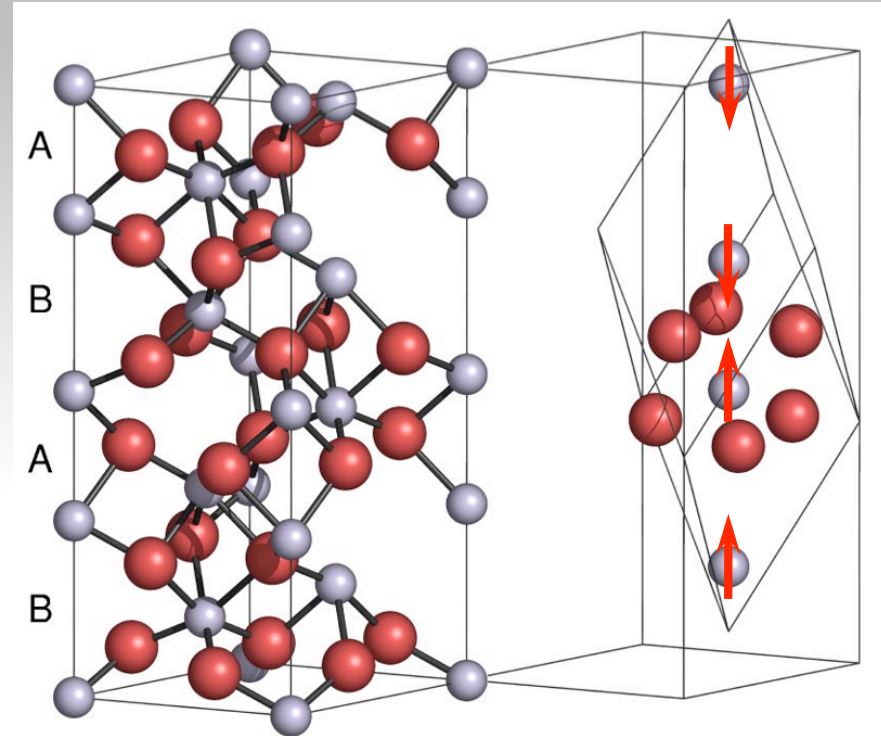- contains the microscopic information

(Gonze and Lee 1997; Baroni et al. 2001)

Hematite (α-Fe$_2$O$_3$)

Rhombohedral symmetry

Antiferromagnetic (T < 260 K)

Highway on a hematite-coloured soil,
Bolivia (Cornell and Schwertmann 2003)

GGA (PBE) + U (3.3 eV)
Ultrasoft pseudopotentials
Wavefunctions cutoff = 40 Ry
4x4x4 k-points

QUANTUMESPRESSO

DFT+U needed to describe correctly electronic and magnetic properties

	GGA	GGA+U	Exp
a_{hex}	5.023	5.098	5.035
c_{hex}	13.901	13.946	13.747
c_{hex}/a_{hex}	2.77	2.74	2.73
mag. mom. (μ_B)	3.87	4.19	4.6–4.9
Band gap (eV)	0.7	1.5	2.0

Theoretical vs. experimental frequencies of transverse optical modes

Blanchard et al. (2008, Am Miner)

200 nm   EHT = 15.00 kV   Signal A = InLens   Photo No. = 2   Mag = 100.00 K X
           WD = 10 mm   Date :25 Apr 2008   Mag Ref To = Monitor   Hématite
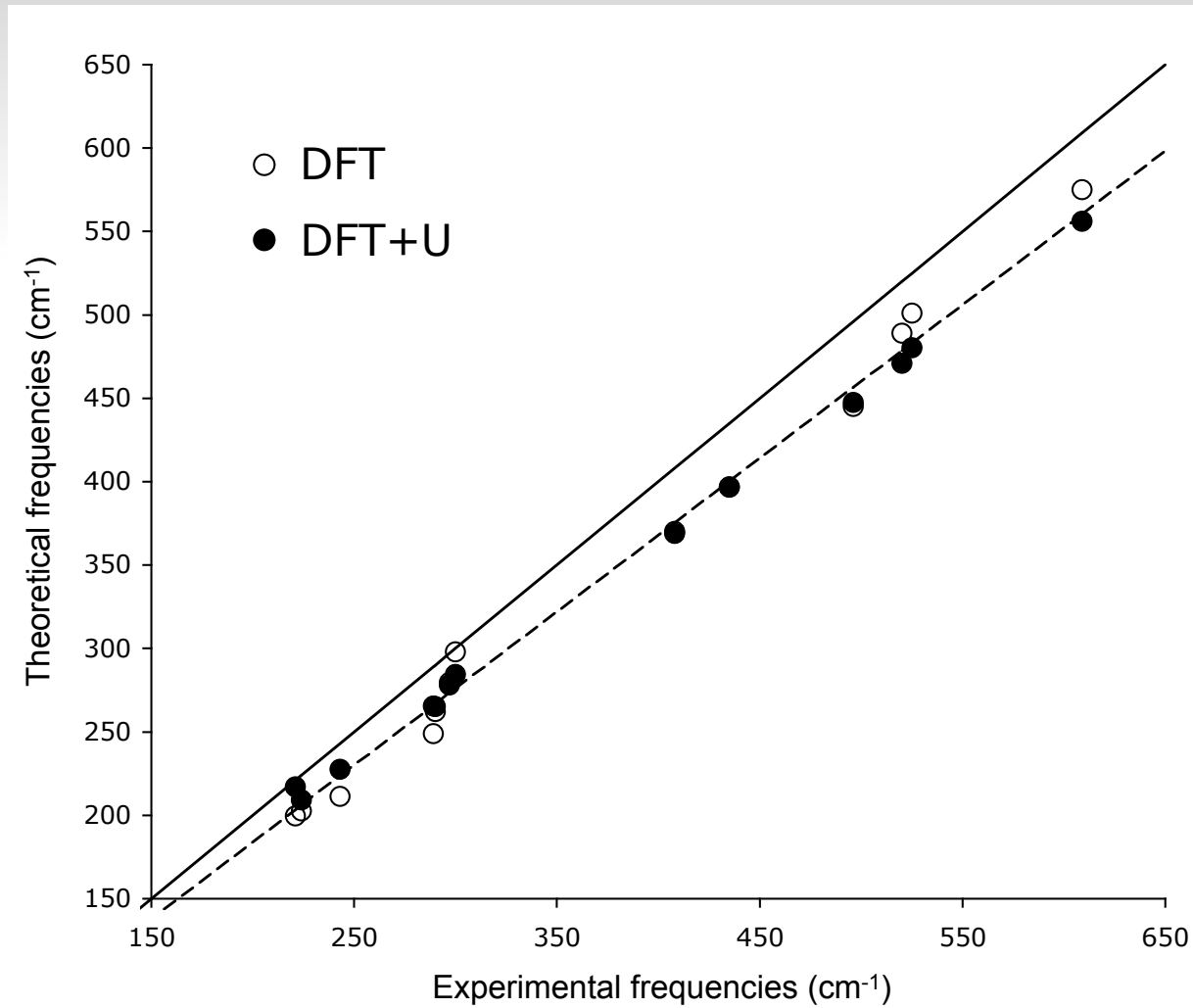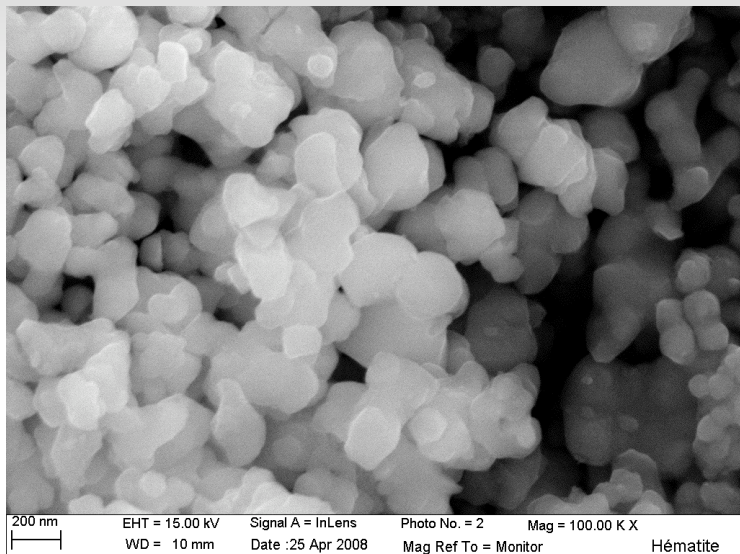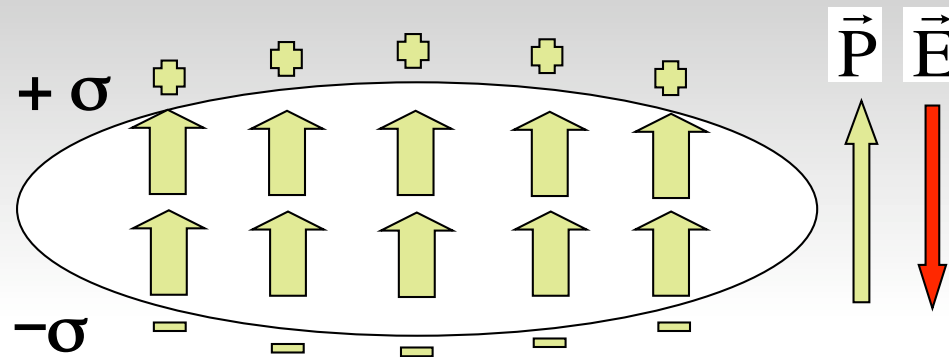
Less than 1 wt. % of powder sample
is diluted in a non-absorbing matrix
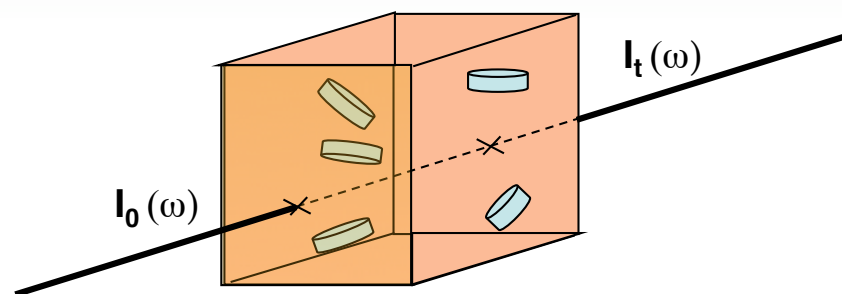
Model:
- ellipsoidal particles
- isolated particles in homogeneous external medium (KBr)
- particle size $< \lambda_{IR}$ (0.74 – 300 µm)

IR absorption depends on the internal macroscopic electric field
(≠ applied electric field)

The electric field induced by surface charges in the polarized
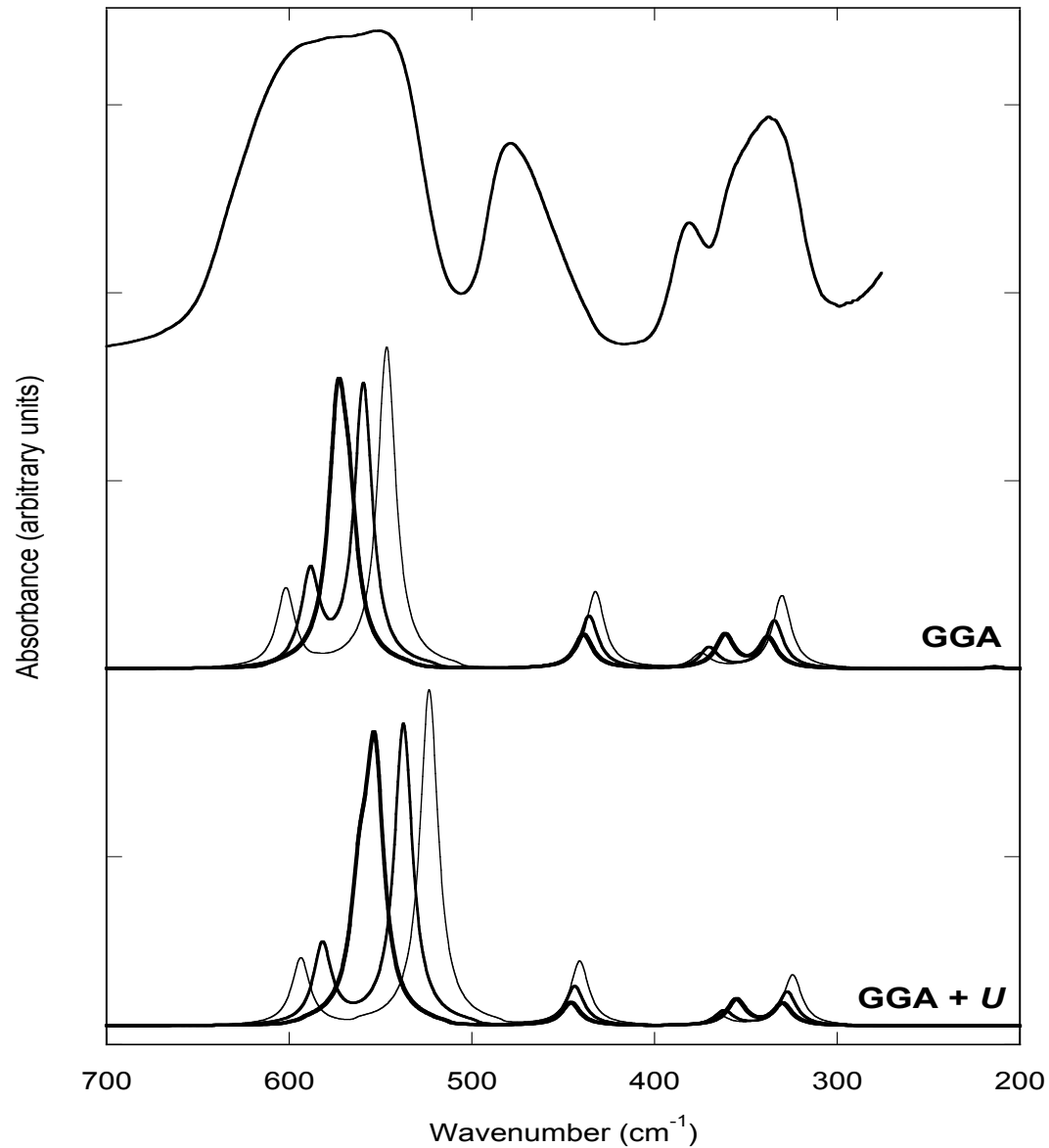particles shifts the absorption bands and affects their intensity

$A(\omega)$ proportional to the orientational and temporal average of
the electromagnetic power dissipated in the particles ($W(\omega)$).

$W(\omega)$: function of the external electric field E_{KBr}, and
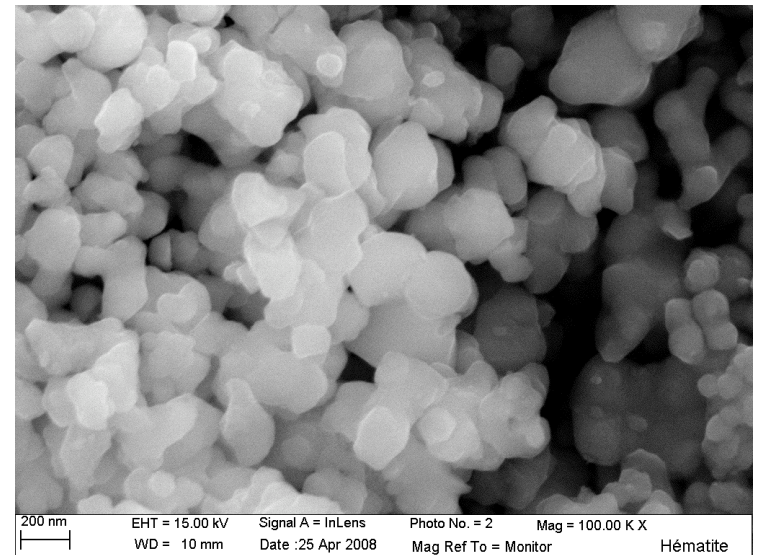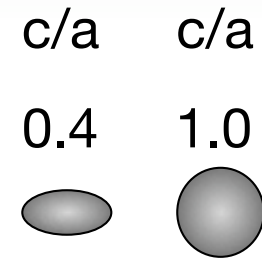dielectric tensors of the sample $\varepsilon(\omega)$ and external medium ε_{KBr}

$$W(\omega) \propto |E_{KBr}|^2 \, \omega \, \mathrm{Im}[\varepsilon(\omega) - \frac{\mathbf{n}.(\varepsilon(\omega) - \varepsilon_{KBr})^2.\mathbf{n}}{(3 \, \mathbf{n}.\varepsilon(\omega).\mathbf{n})}]$$

Effects related to particle shape in the IR spectrum of hematite

Blanchard et al. (2008, Am Miner)

Experimental (top) and theoretical (bottom) IR powder absorption spectra of hematite
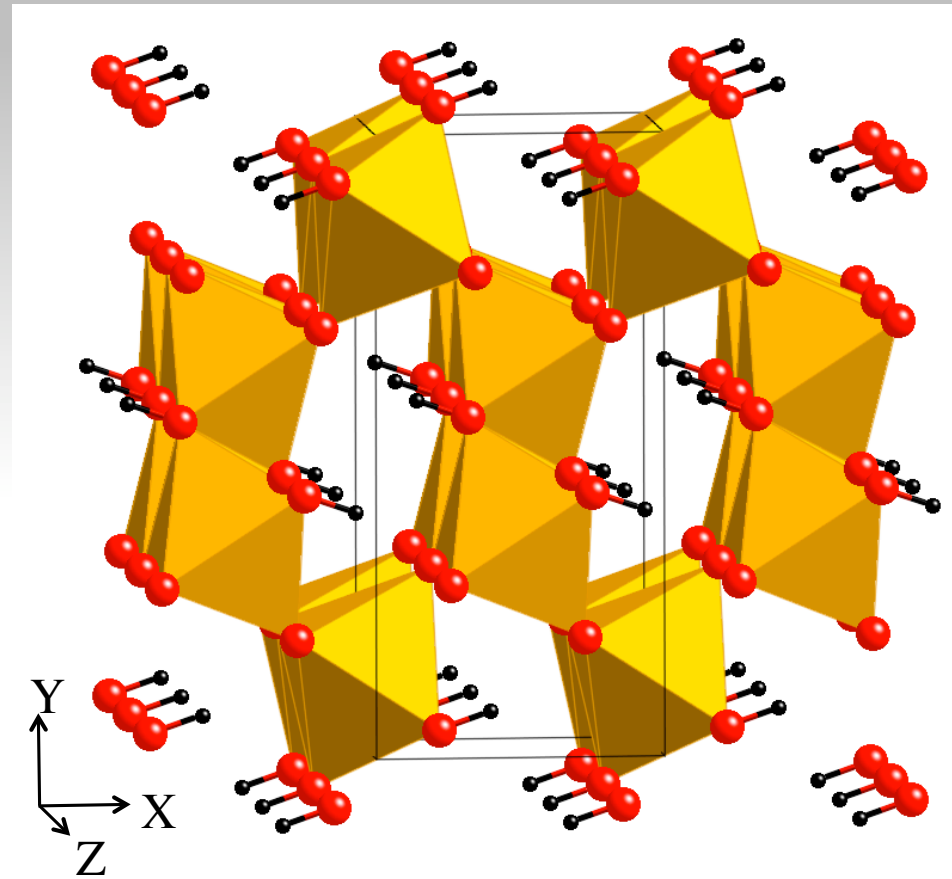
c/a 0.4   c/a 1.0

Broadening related to non-ellipsoidal particles and distribution of particle shapes.

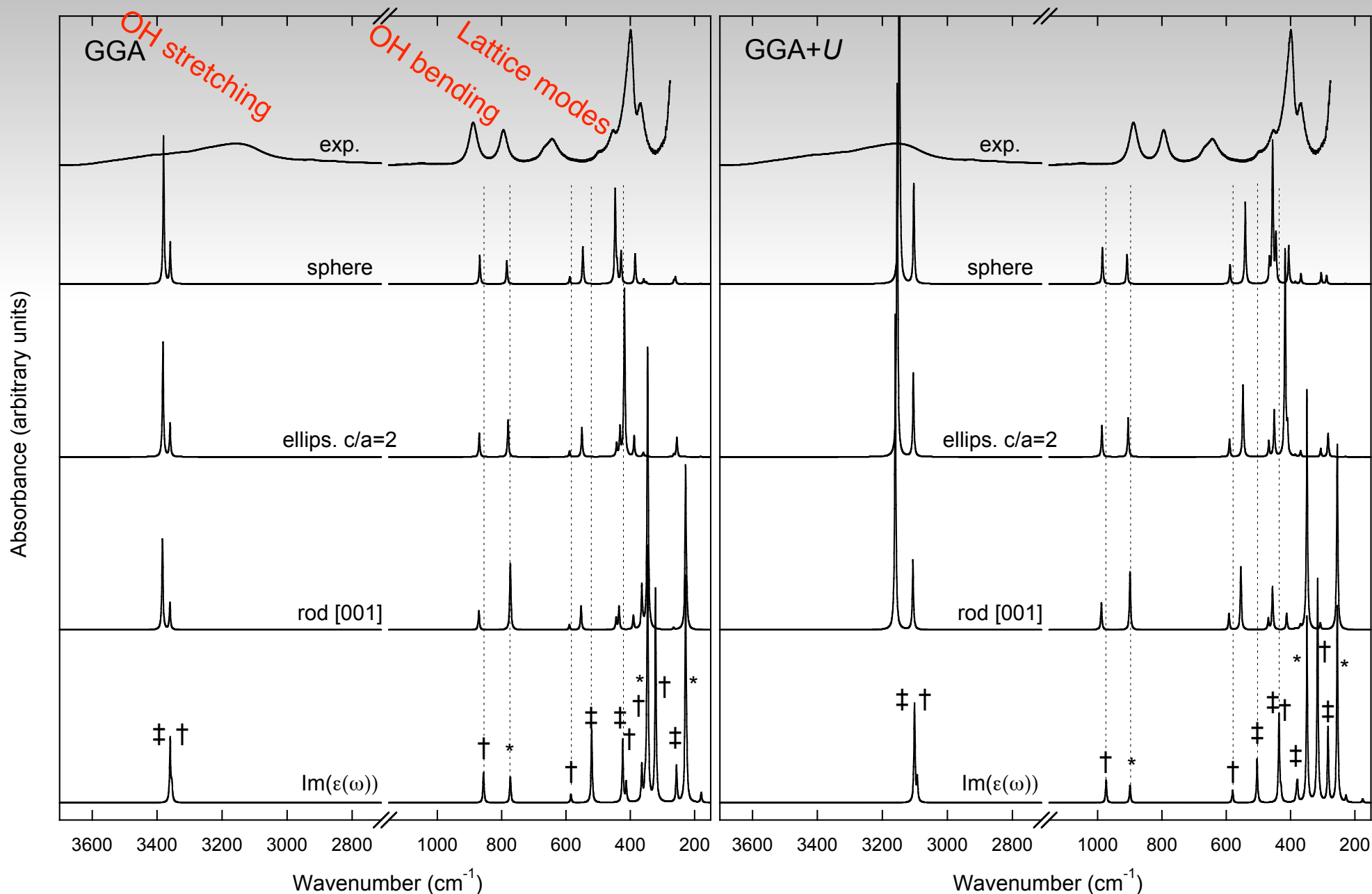Blanchard et al. (2008, Am Miner)

Goethite (α-FeOOH)

Orthorhombic unitcell (*Pbnm*)

GGA (PBE) + U (3.3 eV)
Ultrasoft pseudopotentials
Wavefunctions cutoff = 40 Ry
4x2x6 *k*-points

QUANTUM**ESPRESSO**

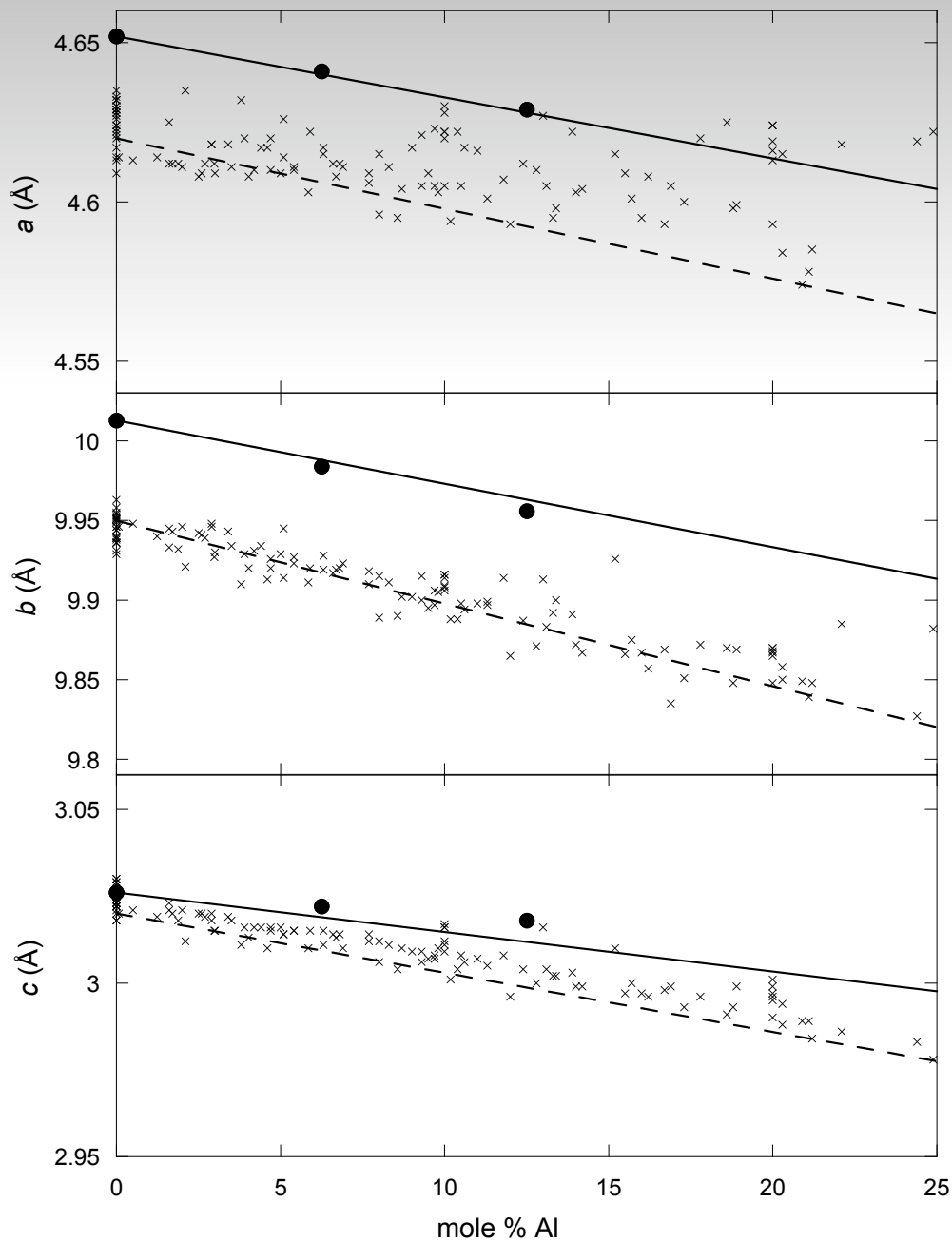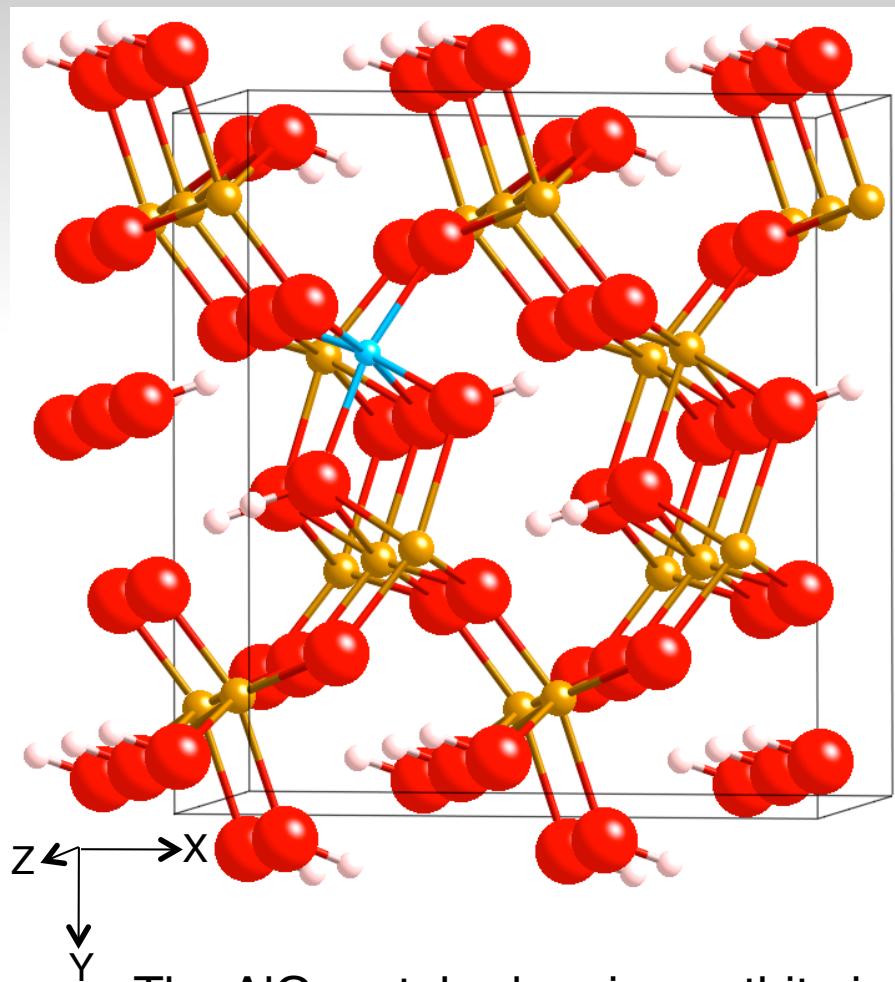|	a	b	c
Goeth. GGA	4.652	10.013	3.026
Goeth. GGA+U	4.638	10.085	3.067
Exp. (Yang et al. 2006)	4.598	9.951	3.018

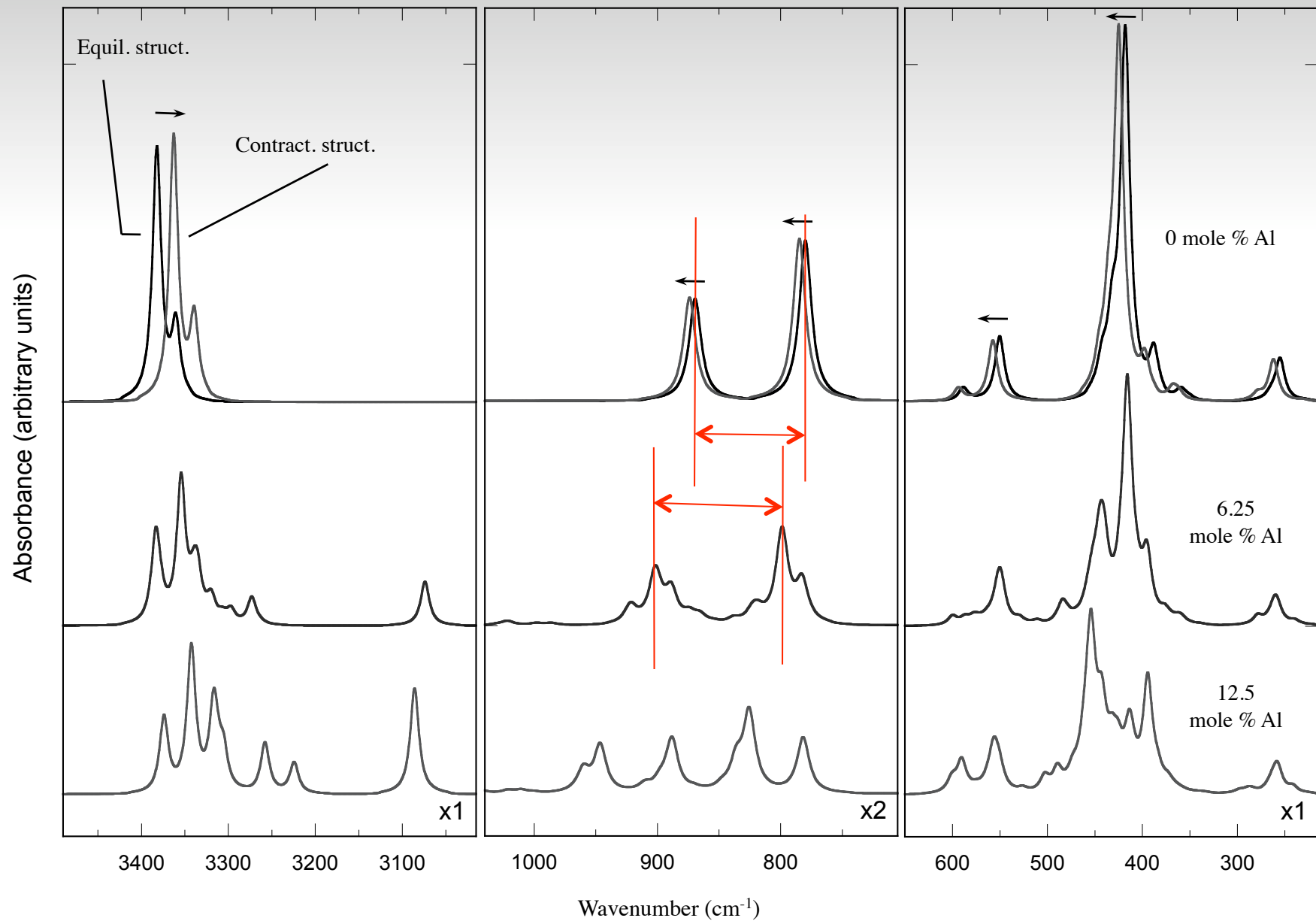Experimental (top) and theoretical (bottom) IR powder absorption spectra of goethite

*, † and ‡ for B_{1u}, B_{2u} and B_{3u} symmetries, respectively

Blanchard et al. (PCM, under review)

Experimental and theoretical (GGA) lattice parameters of goethite versus Al content

The AlO$_6$ octahedron in goethite is sensibly the same as in diaspore (i.e. almost full relaxation)

Effect of the Al substitution on the theoretical (GGA)
IR absorption spectrum of goethite

Conclusions I

- First-principles methods accurate enough to enable a direct comparison with experiment

- A single theoretical framework to interpret the results of various spectroscopic measurements (IR, Raman, NMR, XAS, ...) on complex samples

- Microscopic vs. macroscopic effects in IR powder spectra

X isotope exchange between two phases A and B:

$$AX + BX^* \leftrightarrow AX^* + BX$$

AX

BX

Δ_A Δ_B
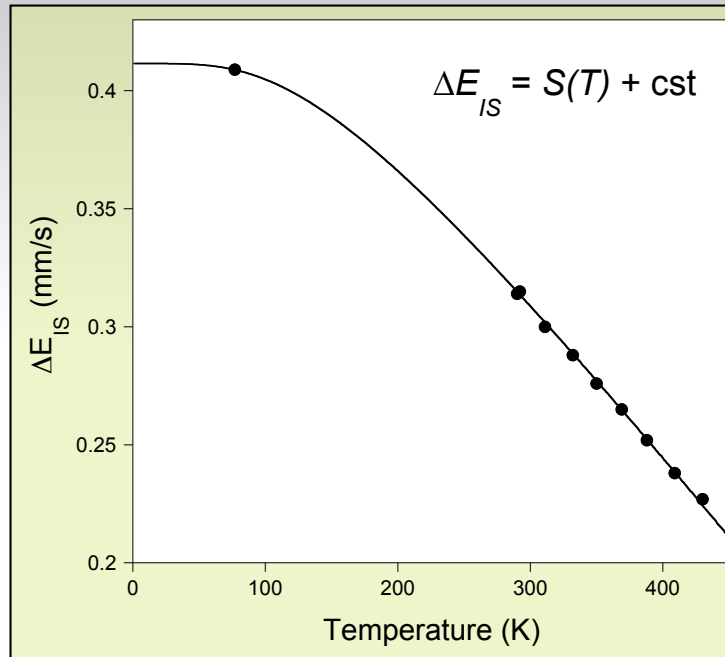
F

AX*

BX*
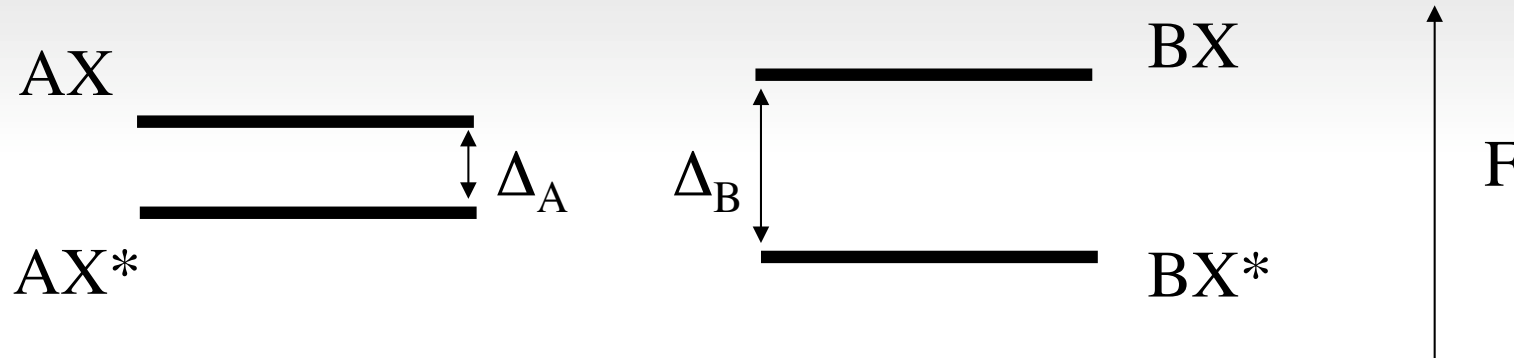
$$\ln(K) = (\Delta_A - \Delta_B)/kT$$

$$F = -kT \ln(Q) \Rightarrow K = (Q_{AX^*}/Q_{AX})/(Q_{BX^*}/Q_{BX})$$

For a crystal, the partition function is: $Q = \left[\prod_{i=1}^{3Nat} \prod_{\{q\}} \frac{e^{-h\nu_{q,i}/(2kT)}}{1 - e^{-h\nu_{q,i}/(kT)}} \right]^{1/N_q}$

β-factor = equilibrium isotopic fractionation factor between phase A and an ideal gas of X

From 1st order thermodynamic perturbation theory:

$$\ln \beta = \frac{m^* - m}{m} \left(\frac{K}{RT} - \frac{3}{2} \right)$$

$$\Delta E_{IS} = S(T) + cst$$

In **Mössbauer**, the kinetic energy of the iron sublattice is related to the second-order Doppler shift (*S(T)*)
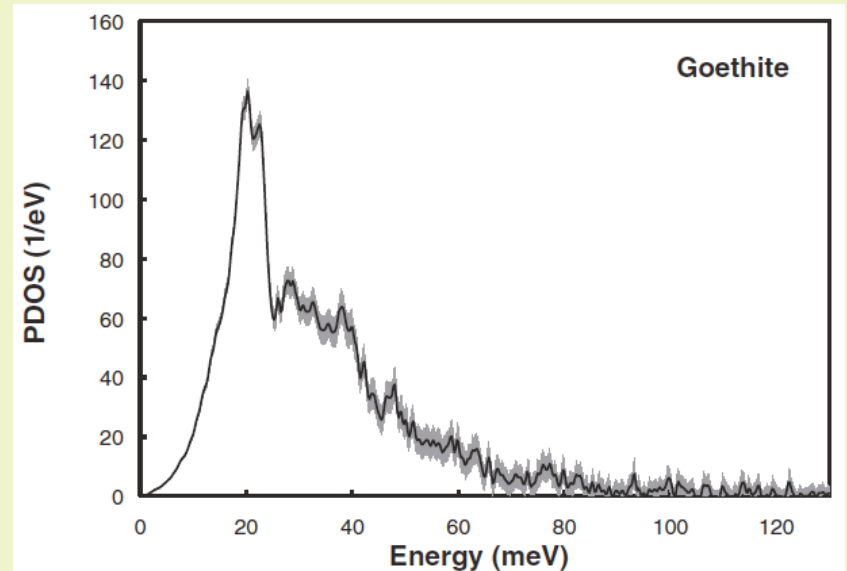
$$S(T) = -\frac{K(T)_{57Fe}}{m\,c}$$

velocity of light

In **Nuclear Resonant Inelastic X-ray Scattering (NRIXS)**, the kinetic energy is related to the partial vibrational density of state (PDOS)

$$K_{57Fe} = \frac{3}{2} \int_0^{e_{max}} E(e,T)g(e)\,de$$
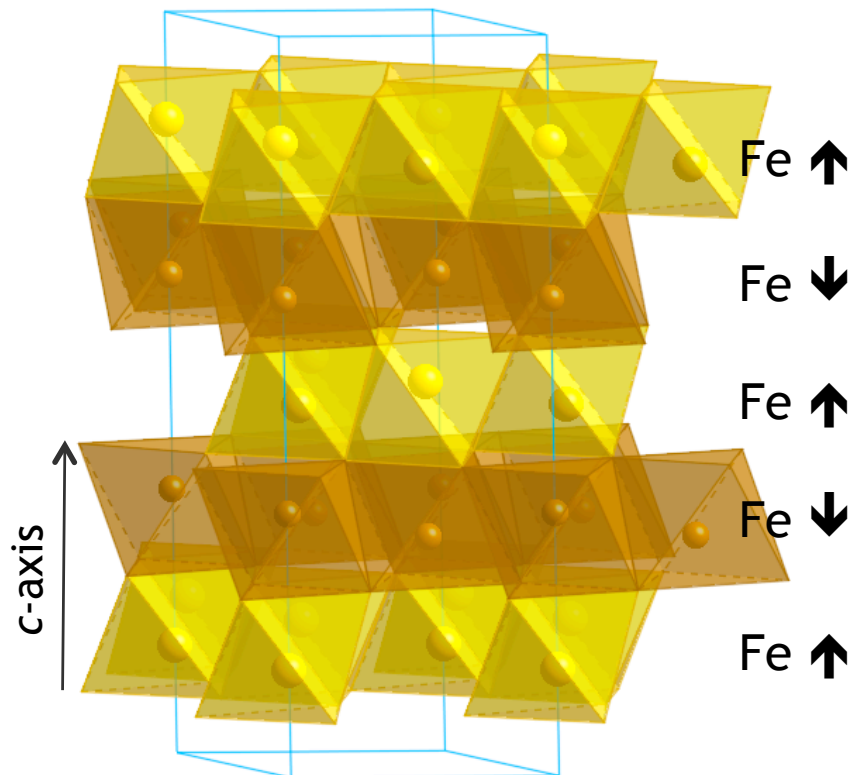
Einstein function   PDOS norm. to 1

- Density Functional Theory

(Plane-waves / Ultrasoft pseudopotentials / Experimental cell parameters / GGA+U)

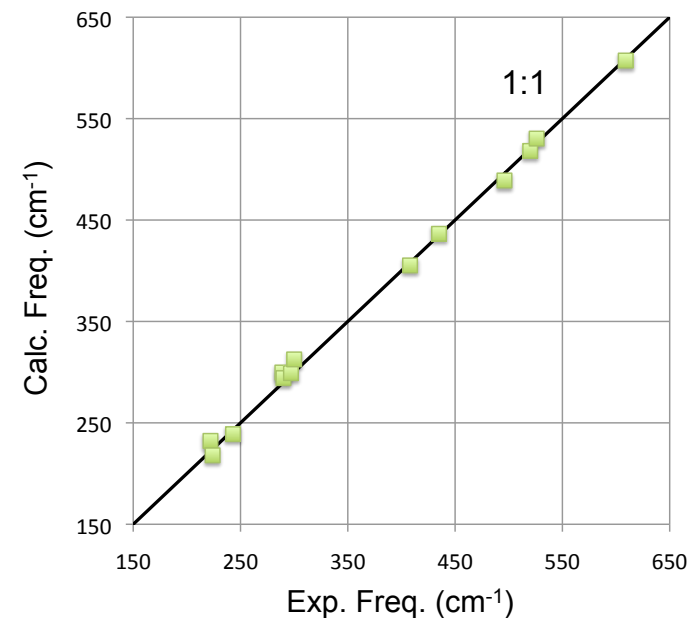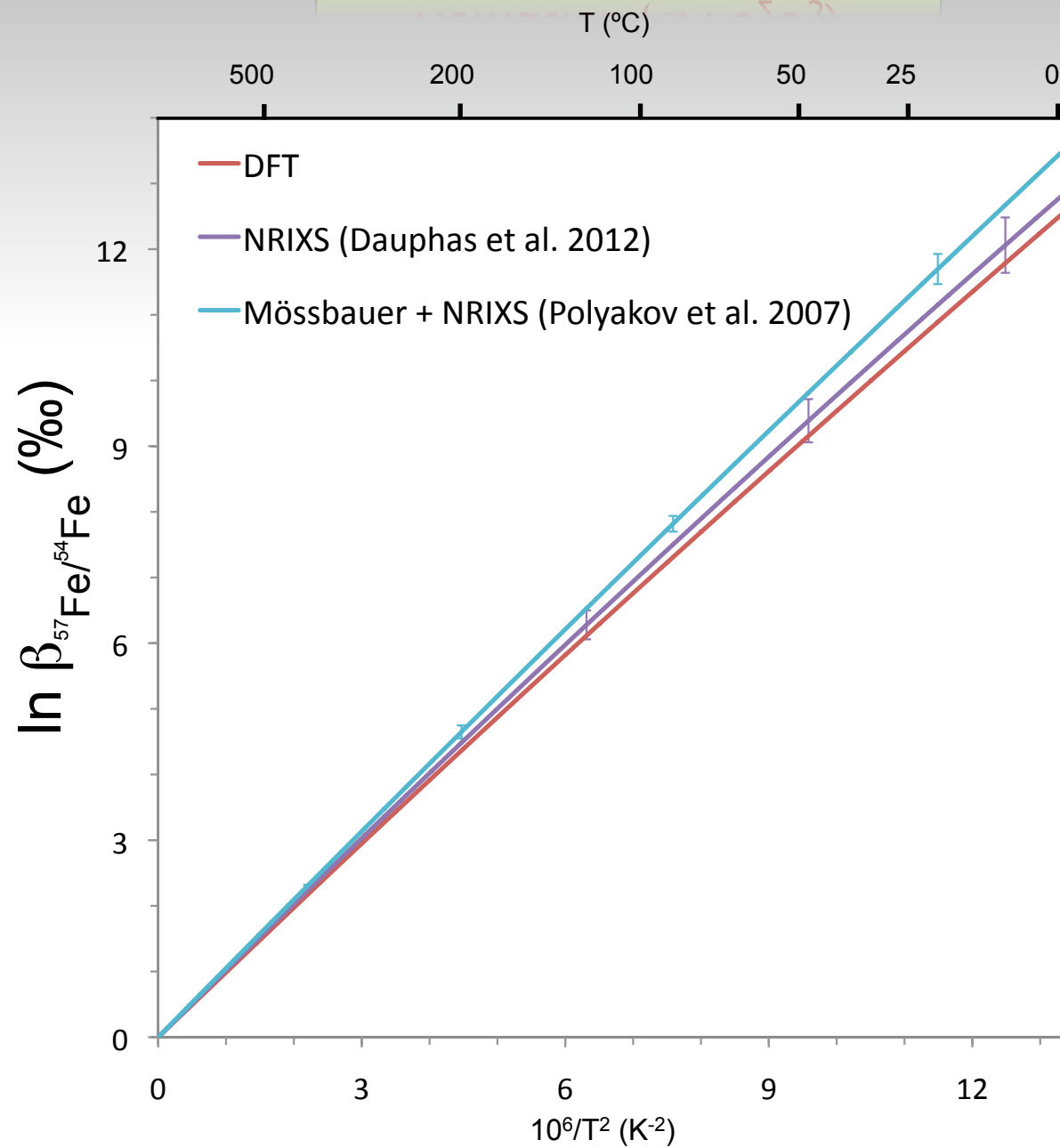- Hematite (α-Fe_2O_3), hexagonal sym., antiferromagnetic

Atomic positions

	x_{Fe}	x_O
Calc.	0.1449	-0.0558
Exp.	0.1447	-0.0556

Raman and IR frequencies

Fe ↑

Fe ↓

Fe ↑

Fe ↓

Fe ↑

c-axis
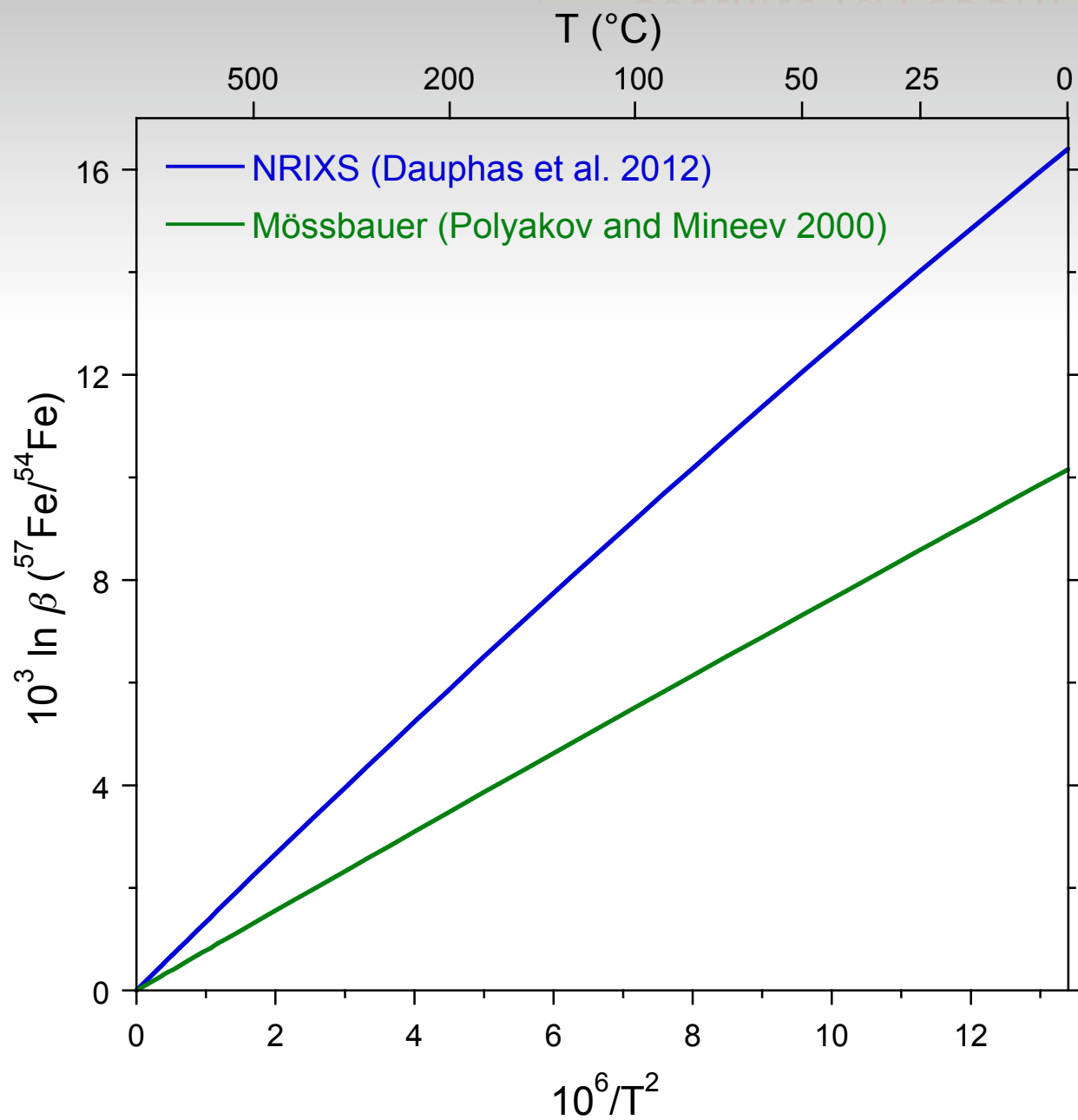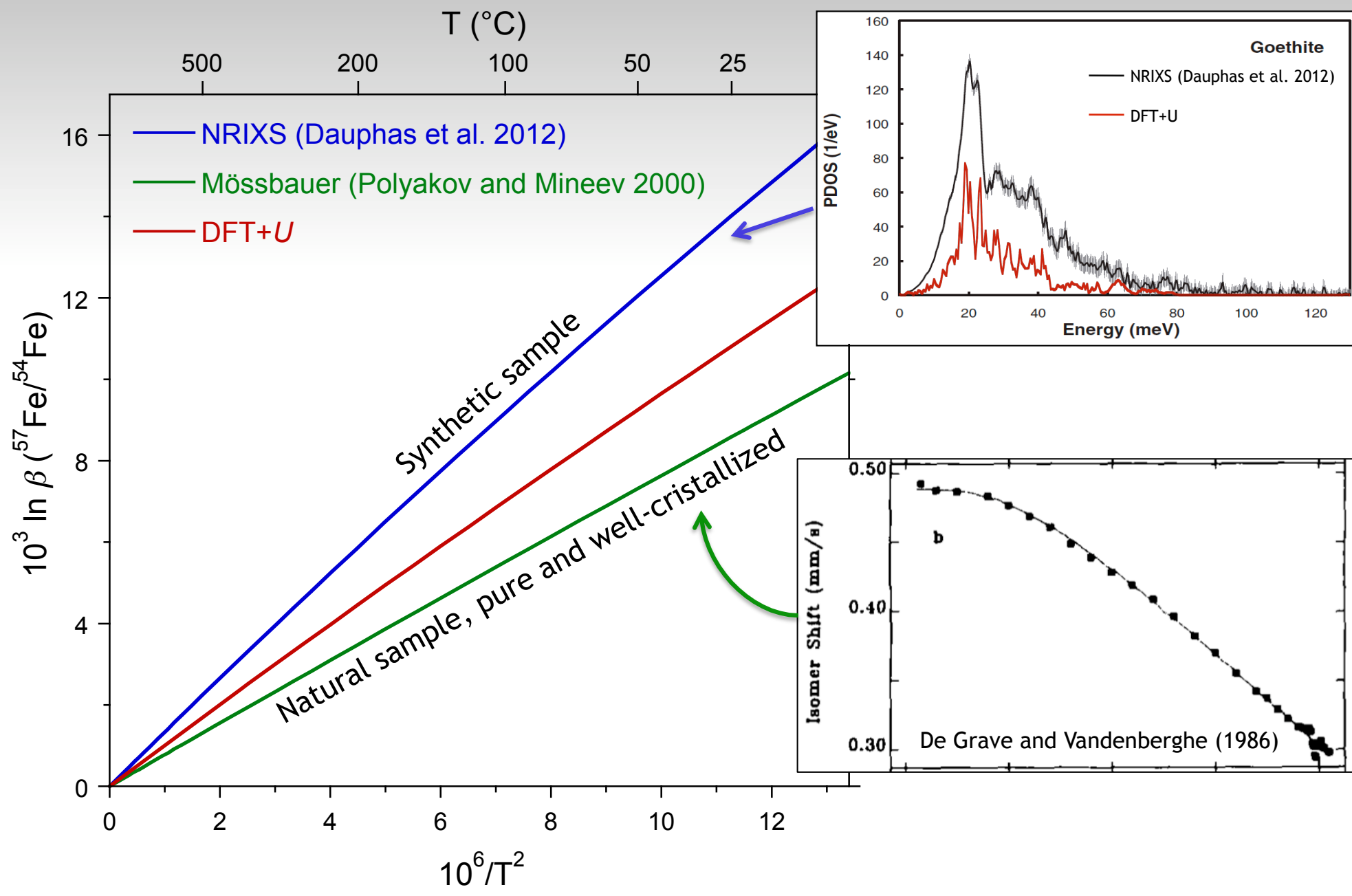
Compositions investigated

Highest Fe β of the structure

Al

c-axis
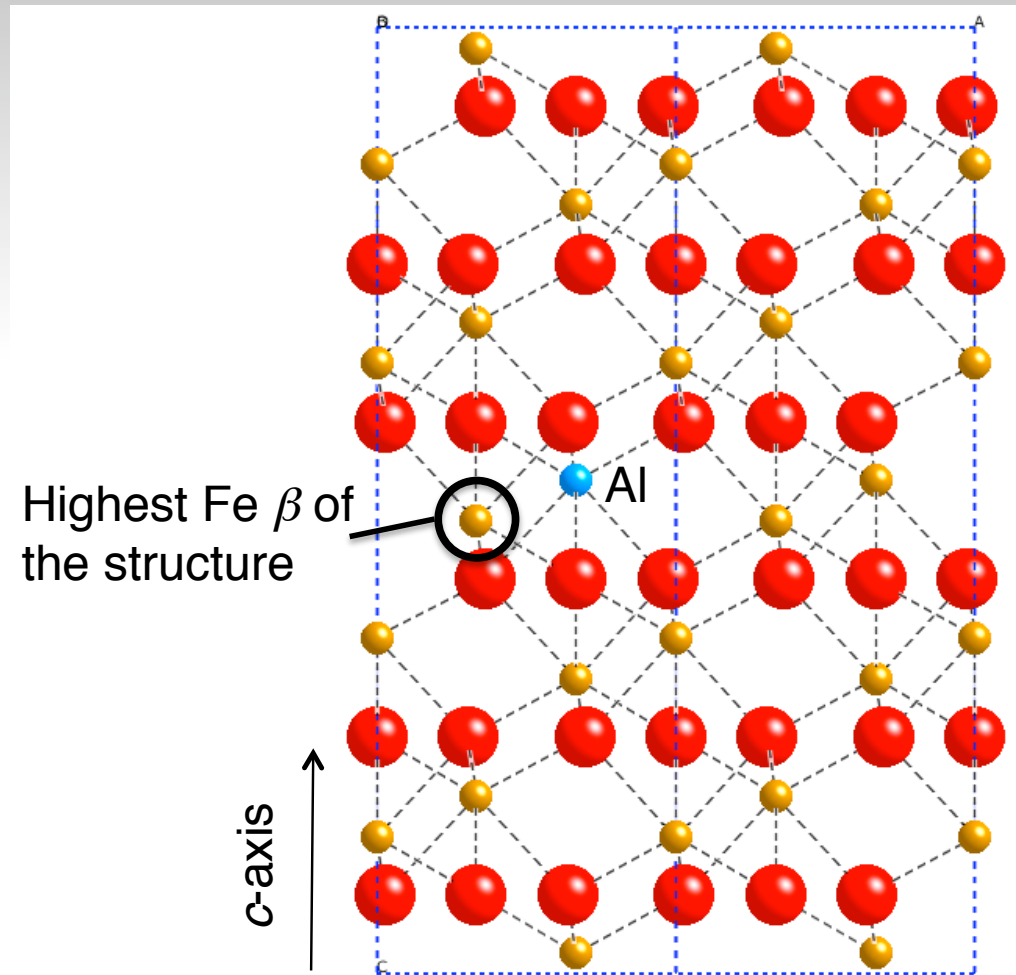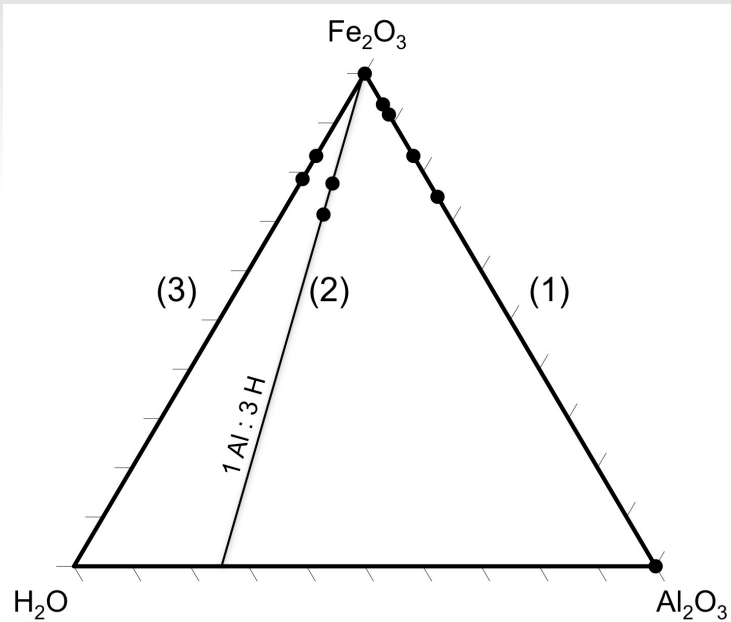
The iron β is higher for Fe atoms located next to the Al impurity.
The effect is larger when Al is in the edge-sharing octahedron rather than in the corner-sharing or face-sharing octahedron.

Oxygen β-factor of hematite vs Al or H content

At 0°C

Al-substituted hematite

H-bearing hematite

$10^3 \ln \beta \, (^{18}O/^{16}O)$

mole % Al_2O_3 or H_2O
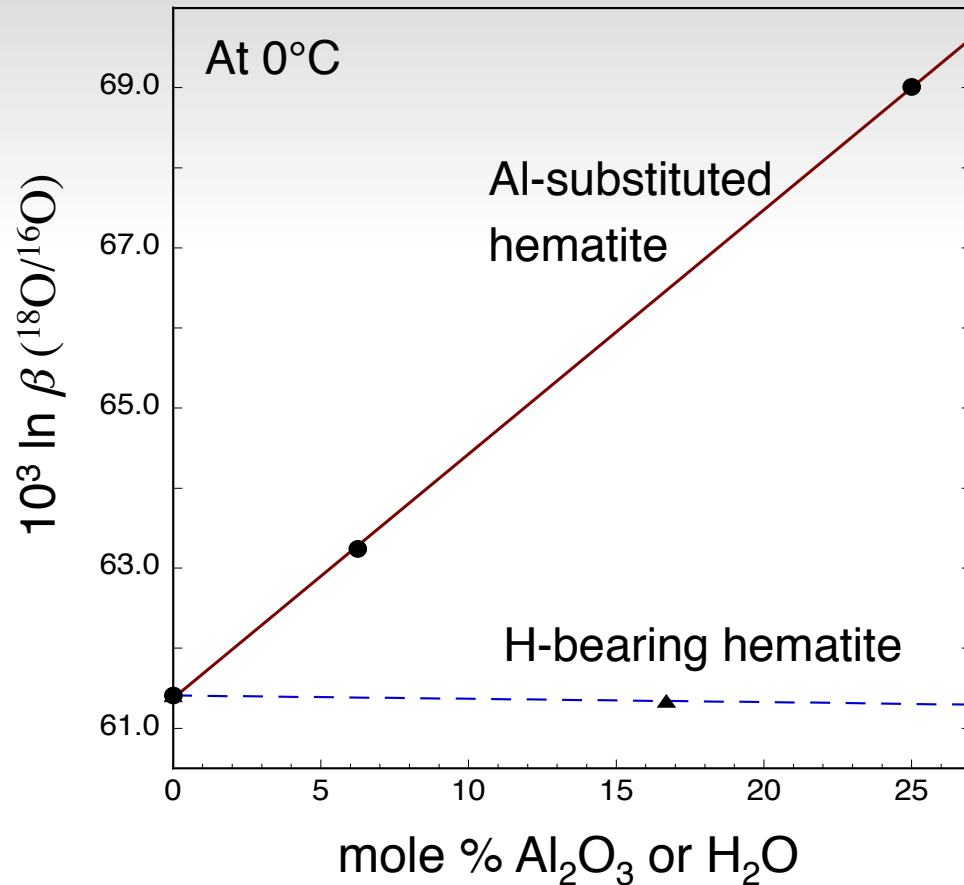
- An incorporation of 18 mole % Al_2O_3 in hematite would increase the oxygen β of ~5.5‰ at 0°C. This effect is sufficiently large to be measurable and to affect the interpretation of natural isotopic compositions.

- The effect of H incorporation is found to be negligible. This is explained by a complex local relaxation of the defective structure leading to a compensation of local β values.

Conclusions II

• Comparing the data obtained from the different techniques (DFT, Mössbauer, NRIXS) enables to obtain reliable equilibrium isotopic fractionation factors.

• First-principles calculations also allow to investigate the mechanisms controlling isotopic fractionations at the molecular scale (crystallographic sites, surface effect, adsorption processes …)

Acknowledgements